



NKS-366  
ISBN 978-87-7893-451-2

---

# CFD simulations of preliminary single spray experiments

Timo Pättikangas and Risto Huhtanen

VTT Technical Research Centre of Finland

June 2016

## **Abstract**

The single spray nozzle experiments performed at the Lappeenranta University of Technology (LUT) are modelled with CFD calculations. The spray droplets are described by using the Discrete Particle Model of the ANSYS Fluent code. Suitable model for the size distribution of the droplets is chosen from the models available in Fluent. Single spray nozzle experiments performed at LUT are modelled and the CFD calculations are compared to available experimental results. The results will be used for the modelling of the spray experiments performed with the PPOOLEX facility at LUT.

## **Key words**

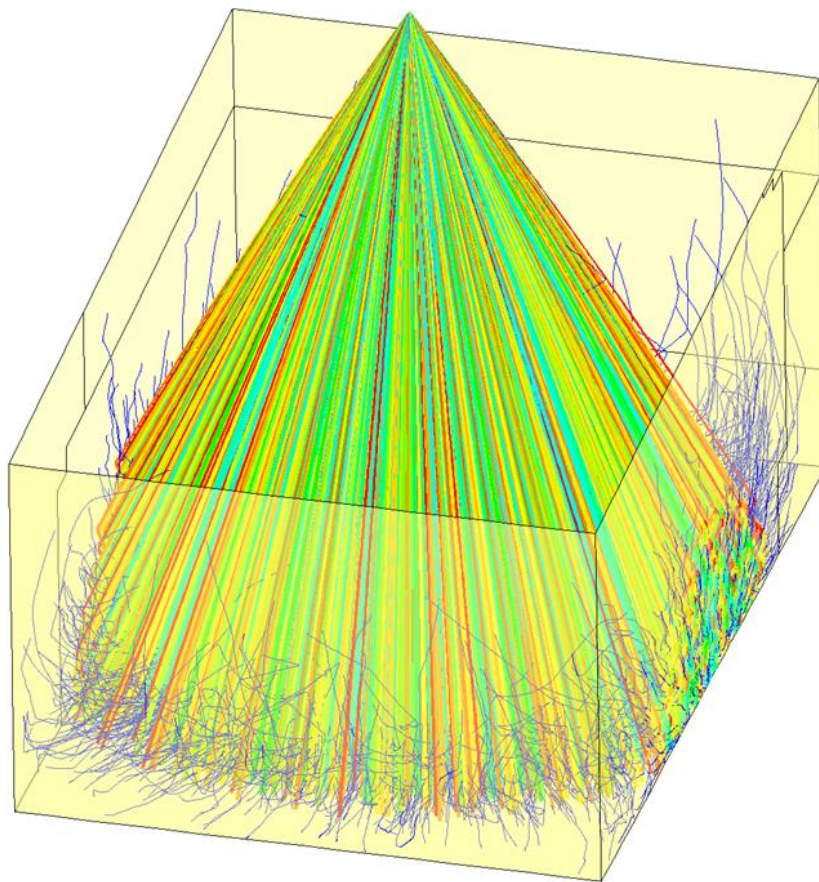
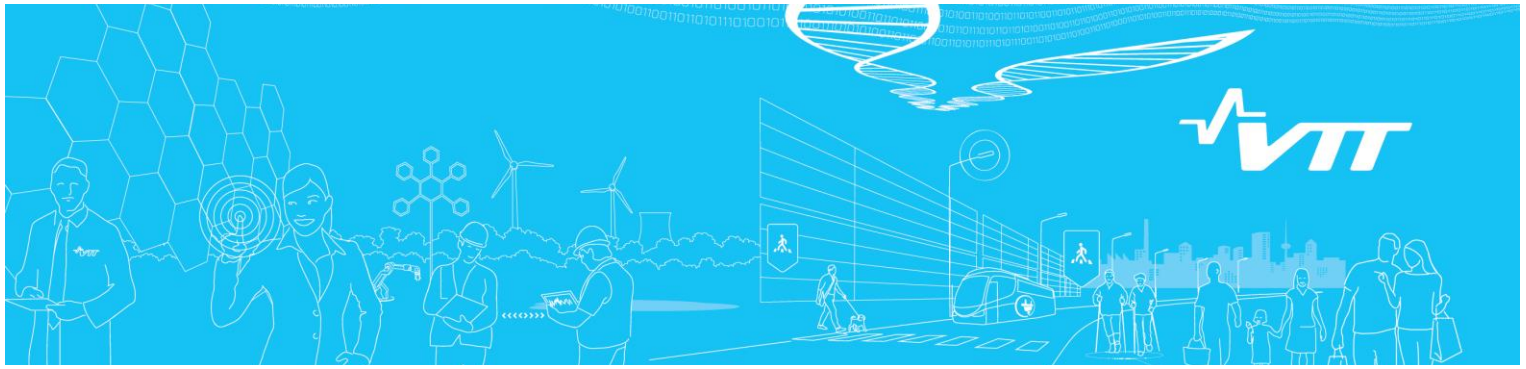
Spray, droplet, containment, nuclear reactor safety, NRS, computational fluid dynamics, CFD

## **Acknowledgment**

NKS conveys its gratitude to all organisations and persons who by means of financial support or contributions in kind have made the work presented in this report possible.

## **Disclaimer**

The views expressed in this document remain the responsibility of the author(s) and do not necessarily reflect those of NKS. In particular, neither NKS nor any other organization or body supporting NKS activities can be held responsible for the material presented in this report.



# **CFD simulations of preliminary single spray experiments**

Authors: Timo Pättikangas and Risto Huhtanen

Confidentiality: Public



<b>Report's title</b>	
CFD simulations of preliminary single spray experiments	
<b>Customer, contact person, address</b>	<b>Order reference</b>
1. Valtion ydinjätehuoltorahasto, Työ- ja elinkeinoministeriö, PL 32, 00023 VALTIONEUVOSTO 2. Nordic nuclear safety research (NKS), Karin Andgren, Programme Manager NKS-R, VATTENFALL, SE-169 92 Stockholm, SWEDEN	1. SAFIR2018 Programme: Dnro SAFIR 14/2015 2. NKS Contract no. AFT/NKS-R(15)114/3
<b>Project name</b>	<b>Project number/Short name</b>
Development and validation of CFD methods for nuclear reactor safety assessment	104836 / NURESA
<b>Author(s)</b>	<b>Pages</b>
Timo Pättikangas and Risto Huhtanen	32 p.
<b>Keywords</b>	<b>Report identification code</b>
Spray, droplet, containment, nuclear reactor safety, NRS, computational fluid dynamics, CFD	VTT-R-05311-15
<b>Summary</b>	
<p>The single spray nozzle experiments performed at LUT are modelled with CFD calculations. The spray droplets are described by using the Discrete Particle Model of the ANSYS Fluent code. Suitable model for the size distribution of the droplets is chosen from the models available in Fluent. Single spray nozzle experiments performed at LUT are modelled and the CFD calculations are compared to available experimental results. The results will be used for the modelling of the spray experiments performed with the PPOOLEX facility at LUT.</p>	
<b>Confidentiality</b>	Public
Espoo, 29 April 2016	
<b>Written by</b>	<b>Reviewed by</b>
	
Timo Pättikangas Principal Scientist	Mikko Manninen Principal Scientist
<b>Accepted by</b>	
	
Lars Kjaldman Research Team Leader	
<b>VTT's contact address</b>	
VTT Technical Research Centre of Finland Ltd, P.O.B. 1000, FI-02044 VTT, Finland	
<b>Distribution (customer and VTT)</b>	
Emma Palm (NKS), STUK, Vesa Suolonen (VTT), Markku Puustinen (LUT), Heikki Purhonen (LUT), Lauri Pyy (LUT), SAFIR2018 Reference Group 4	
<p><i>The use of the name of VTT Technical Research Centre of Finland Ltd in advertising or publishing of a part of this report is only permissible with written authorisation from VTT Technical Research Centre of Finland Ltd.</i></p>	



## Preface

---

This work has been carried out in the Work Package 2 of the NURESA project of the SAFIR2018 programme (The Finnish Research Programme on Nuclear Power Plant Safety). The project has been funded by Valtion ydinjätehuoltorahasto, VTT and NKS (Nordic nuclear safety research). The authors are grateful for comments obtained from the members of the SAFIR2018 Reference Group 4 and from the Northnet Roadmap 3 Reference Group.

Espoo, 30 November 2015

Authors

## Contents

---

Preface.....	3
Contents.....	4
1. Introduction.....	5
2. Estimation of the size distribution of the droplets .....	6
2.1 The plain-orifice atomizer model.....	6
2.2 Operation modes of the spray nozzles.....	7
2.3 Primary breakup distribution of droplets.....	9
3. Simulations of the preliminary single spray test facility.....	11
3.1 Numerical model.....	11
3.2 CFD simulations of the preliminary spray experiments.....	12
4. Simulations of the single spray test facility .....	17
4.1 Numerical model.....	17
4.2 CFD simulations of the first experiments.....	19
5. Summary and discussion.....	23
References.....	24

## 1. Introduction

---

At the Lappeenranta University of Technology (LUT), experiments are performed where the behavior of different spray nozzles is tested (Pyy et al., 2015, 2016). The formation of spray droplets in the nozzles is studied by varying the pressure drop over the nozzle. The size distribution of the droplets is measured with shadowgraphy at different distances from the nozzle. It is planned that sprays will be installed in the PPOOLEX test facility, which is a downscaled model of boiling water reactor containment.

Primary atomization of the liquid jet occurs near the outlet of the nozzle. Turbulent fluctuations of the liquid jet induce perturbations on the jet surface, which grow and break the jet into droplets. The length scale of turbulence is the dominant length scale of atomization, which also determines the resulting droplet size (Chryssakis et al., 2011).

Two different primary breakup distributions are commonly used for describing droplet diameters. In the lognormal distribution, the logarithm of the droplet diameter obeys normal distribution. In the Rosin-Rammler distribution, the diameter distribution is also described with two parameters, i.e., the mean diameter of the droplets and the spread of the distribution (Schick, 2006; Foissac et al., 2013).

After the primary breakup of the liquid jet, the largest droplets may further break into smaller droplets in secondary breakup. Droplet may break if drag force caused by air is large enough to overcome the surface tension of the droplet. Several models for the secondary breakup have been developed. The Taylor Analogy Breakup model compares the oscillations of the droplet caused by drag force to the surface tension in order to determine the breakup. In the Kelvin-Helmholtz breakup model, the growth rate and the wavelength of instability is determined to find characteristic breakup time (Chryssakis et al., 2011; Sazhin, 2014).

The impinging droplets of the spray form liquid films on surrounding walls and floors. The liquid film affect the heat transfer to the walls and the shear forces between the film and gas affect the flow velocity of the gas phase. In addition, impinging of droplets may cause splashing of secondary droplets from the liquid film.

In the present work, the first single spray nozzle experiments performed at LUT are modelled with Computational Fluid Dynamics (CFD) calculations. The traces of an ensemble of spray droplets are solved in a numerical mesh describing the experimental setup. The flow of the surrounding air and its interaction with the droplets is solved by using the control volume method. In the calculations, the primary breakup distribution of the droplets is modelled with the ANSYS Fluent CFD code (ANSYS, 2016).

In the first experiments performed at LUT, full cone spray nozzle (Spraying Systems Co, 2015) with a capacity of 10 liters/min was tested at the preliminary single spray testing station. In the second set of experiments, full cone spray nozzle with a capacity of 40 liters/min was tested at a new single spray testing station. In both experiments, the droplet sizes were measured with shadowgraphy (Pyy et al., 2015, 2016). It is planned that later concentrations of droplets at different parts of the cone are also measured.

In the present report, the estimation of the size distributions of the droplets is discussed in Section 2. The main features of the plain-orifice atomizer model are presented and the model is applied to the spray nozzles used in the experiments. The Sauter mean diameters of the droplets are estimated and the primary breakup distribution is described with the Rosin-Rammler distribution. In Section 3, the simulation of an experiment performed for the preliminary single spray test facility is presented. In this experiment, the smallest spray nozzle with a capacity of 10 liters/min was used. In Section 4, the simulation of an experiment performed at the newly constructed spray testing station is described. The largest spray nozzle with a capacity of 40 liters/min was used in this experiment. Finally, in Section 5 the results are summarized and discussed.

## 2. Estimation of the size distribution of the droplets

Commercial CFD codes have readily available several atomizer models for the description of the primary breakup phenomena after the nozzle. In the following, the simplest atomizer model of ANSYS Fluent (2016) is first briefly described. Then, the average diameter of the droplets produced by the atomizer is determined. Finally, an estimate for the size distribution of the droplets is formed.

### 2.1 The plain-orifice atomizer model

The plain-orifice atomizer is common and simple atomizer. It has three different operation modes, which are illustrated in Figure 1. In the single-phase nozzle flow mode, the liquid completely fills the orifice. In cavitating nozzle flow, vapor pockets form inside the nozzle just after the inlet corners. In flipped nozzle flow, downstream gas surrounds the liquid jet inside the nozzle. The operation mode of the nozzle depends on the dimensions of the nozzle, the pressure difference over the nozzle and the liquid and gas properties.

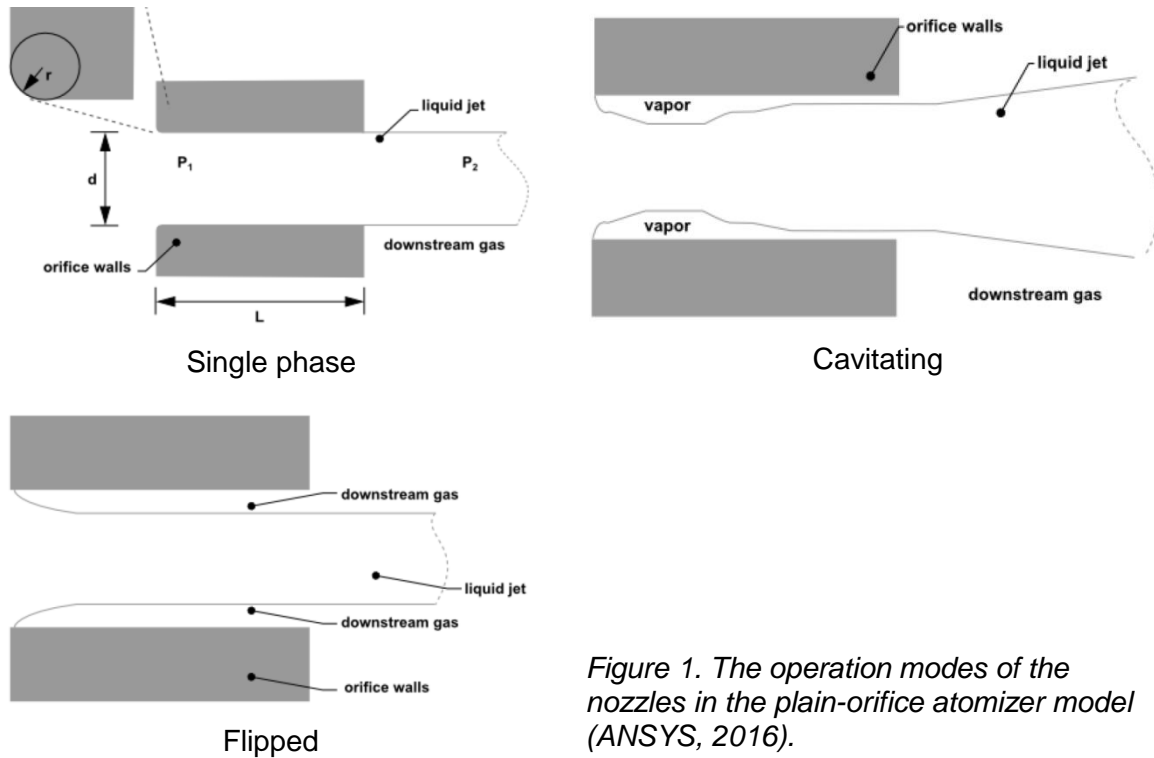


Figure 1. The operation modes of the nozzles in the plain-orifice atomizer model (ANSYS, 2016).

In the plain-orifice atomizer model, the operation mode of the nozzle is determined based on the Reynolds number, the cavitation number and the critical values for the inception of cavitation and flipping (ANSYS, 2016).

The Reynolds number based on hydraulic head is defined as

$$Re_h = (d\rho_l/\mu)\sqrt{2(p_1 - p_2)/\rho_l} \quad (1)$$

where  $d$  is the nozzle diameter,  $\rho_l$  is the liquid density and  $\mu$  is the liquid viscosity. The upstream and downstream pressures are denoted by  $p_1$  and  $p_2$ , respectively. The cavitation number is defined as

$$K = (p_1 - p_v)/(p_1 - p_2) \quad (2)$$

where  $p_v$  is the vapor pressure.

For short, sharp-edged nozzles, the inception of cavitation occurs approximately at cavitation number  $K_{\text{insep}} \approx 1.9$ . The effect of the rounding of the inlet edge ( $r$ ) and the viscosity are taken into account by the empirical relation for the inception of cavitation (ANSYS, 2016):

$$K_{\text{insep}} = 1.9 \left(1 - \frac{r}{d}\right)^2 - \frac{1000}{\text{Re}_h} \quad (3)$$

Correspondingly, the critical value of the cavitation number, where flip occurs, is given by

$$K_{\text{crit}} = 1 + \left(1 + \frac{L}{4d}\right)^{-1} \left(1 + \frac{2000}{\text{Re}_h}\right)^{-1} \exp\left(\frac{-70r}{d}\right) \quad (4)$$

If the rounding of the inlet edge of the nozzle is large enough ( $r/d > 0.05$ ), flip is considered impossible and we set  $K_{\text{crit}} = 1$ .

The decision tree for the state of the nozzle is shown in Figure 2. The state of the nozzle can be estimated by calculating the cavitation parameter and comparing it to the critical values of the inception of cavitation and flipping. In the following, the decision tree is applied to the nozzles used in single spray nozzle experiments performed at LUT.

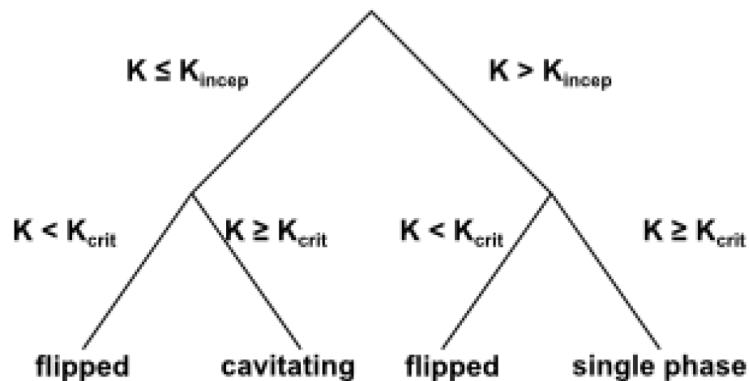


Figure 2. Decision tree for the state of the nozzle in the plain-orifice atomizer model (ANSYS, 2016).

## 2.2 Operation modes of the spray nozzles

In the experiments, full cone nozzles of Spraying Systems Co. (2015) are used. The nozzle B1/4HH-10 was used in the first preliminary single spray experiments and it is shown in Figure 3. The capacity of the nozzle is 10 liters/min. Its orifice has a diameter of 3.2 mm and a length of 23 mm. When the pressure difference over the nozzle is 1 bar, the cavitation number is  $K = 1.99$ . Therefore, the nozzle operates in the single phase mode.

At higher values of the pressure difference of 3...6 bars, the cavitation number for the nozzle B1/4HH-10 is 1.33...1.16. Then, the nozzle is expected to operate in the cavitating or in the flipped mode depending on the rounding radius of the inlet edge of the nozzle. The properties of the nozzle are summarized in Table 1.



Figure 3. Full cone spray nozzle B1/4HH-10 used in the experiments at the preliminary single spray test facility (Spraying Systems Co., 2015).

Table 1. Estimates for the states of used full cone spray nozzles according to the plain-orifice atomizer model.

Nozzle type	Orifice nom. $d$ (mm)	Length $L$ (mm)	$\Delta p$ (bar)	$Re_h$	$K_{incep}$ ( $r/d = 0$ )	$K_{crit}$ ( $r/d = 0$ )	$K$	Mode
B1/4HH-10	3.2	23	1	40 400	1.88	1.34	1.99	Single-phase
			3	69 900	1.89	1.35	1.33	Cavitating ( $r/d > 0.05$ ), Flipped ( $r = 0$ )
			6	98 900	1.89	1.35	1.16	Cavitating ( $r/d > 0.05$ ), Flipped ( $r = 0$ )
B3/8HH-SS22	4.5	24	1	58 200	1.88	1.41	1.99	Single-phase
B1/2HH-40	6.2	30	1	78 200	1.89	1.44	1.99	Single-phase
			6	191 600	1.89	1.45	1.16	Cavitating ( $r/d > 0.05$ ), Flipped ( $r = 0$ )

In later experiments, the larger nozzle B1/2HH-40 having the capacity of 40 liters/min was used. Its orifice has a diameter of 6.2 mm and a length of 30 mm. When the pressure difference over the nozzle is 1 bar, the cavitation number is also for this nozzle  $K = 1.99$ . Therefore, this nozzle is also expected to operate in the single phase mode. At a higher pressure difference of 6 bars, the nozzle operates either in the cavitating or in the flipped mode.

### 2.3 Primary breakup distribution of droplets

Estimates for the average diameter of the droplets after the primary breakup are available in literature. The experimental correlations are based on the Weber number (Brennen, 2005)

$$We = \frac{\rho_l u^2 \lambda}{\sigma} \quad (5)$$

For a single-phase nozzle, the exit velocity of the liquid from the nozzle is  $u = \dot{m}/(\rho_l A)$ , where  $A$  is the nozzle area and  $\dot{m}$  is the mass flow rate. The surface tension is denoted by  $\sigma$  and the radial integral length scale is  $\lambda = d/8$ .

Assume a single-phase nozzle and consider the primary breakup distribution of droplets. An estimate for the Sauter mean diameter of droplets has been presented by Wu et al. (1992):

$$d_{32} = 133 \lambda We^{-0.74} \quad (6)$$

The Sauter mean diameter is the diameter of a sphere that has the same volume to surface area ratio as the total volume of all the drops to the total surface area of all the drops. The most probable droplet diameter is

$$d_0 = 1.27 d_{32} \left(1 - \frac{1}{n}\right)^{1/n} \quad (7)$$

where  $n = 3.5$  is the spread parameter for a single-phase nozzle (ANSYS, 2016).

The size distribution of droplets is often described with the Rosin-Rammler density function (Schick, 2006; Lefebvre, 1989). The Rosin-Rammler density function for the volume (mass) of droplets is

$$f(d^3) = \frac{n}{d_0} \left(\frac{d}{d_0}\right)^{n-1} \exp\left[-\left(\frac{d}{d_0}\right)^n\right] \quad (8)$$

The Rosin-Rammler distribution is readily available in ANSYS Fluent (ANSYS, 2016).

Another alternative for describing the droplet sizes is the lognormal density function (Schick, 2006; Lefebvre, 1989). The lognormal density function for the volume (mass) of droplets is

$$f(d^3) = \frac{1}{\sqrt{2\pi}\sigma d} \exp\left\{-\frac{[\ln(d) - \ln(d_{\text{mean}})]^2}{2\sigma^2}\right\} \quad (9)$$

The lognormal distribution has, for instance, been used by Foissac et al. (2013) for the description of hollow cone sprays of PWR containment.

In the following, we consider the nozzles of Table 1, when the pressure difference over the nozzle is 1 bar. Then, the nozzles operate in the single-phase mode and the estimate in Eq. (6) for the Sauter mean diameter can be used. Comparison of the Rosin-Rammler and lognormal distributions showed that the difference between the distributions is not significant

if suitable parameters for the distributions are chosen. In the following, the Rosin-Rammler density function is used for the size distribution of droplets.

The most probable droplet diameters and the Sauter mean diameters for the nozzles are summarized in Table 2. The corresponding size distributions are shown in Figure 4.

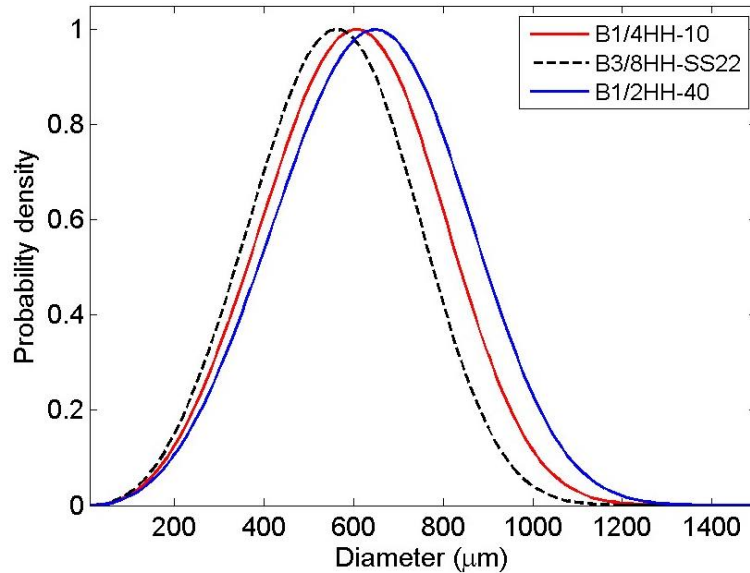


Figure 4. Rosin-Rammler distribution for the volume (mass) of droplets for three nozzles, when the pressure difference over the nozzle is 1 bar. Single phase operation is assumed with a spread parameter of  $n = 3.5$ . The maximum values have been normalized to one.

Table 2. Estimated Sauter mean diameters and the most probable diameters for the spray droplets.

Nozzle type	Orifice nom. $d$ (mm)	Length $L$ (mm)	$\Delta p$ (bar)	$\dot{V}$ (l/min)	$v = \dot{V}/A$ (m/s)	We (-)	$d_{32}$ ( $\mu\text{m}$ )	$d_0$ ( $\mu\text{m}$ )
<b>B1/4HH-10</b>	3.2	23	1	4.4	9.12	452	577	667
<b>B3/8HH-SS22</b>	4.5	24	1	9.7	10.18	792	536	619
<b>B1/2HH-40</b>	6.2	30	1	17.8	9.80	1 010	617	713

### 3. Simulations of the preliminary single spray test facility

At LUT, two experimental series with spray nozzles have been performed (Pyy et al., 2015; Pyy et al., 2016). First, a few tests with the preliminary single spray test facility were performed, where the measurement of droplet sizes with shadowgraphy was piloted. Second, a test station for the spray experiments was constructed, where a test series was performed. In the following, the CFD simulations of the first preliminary tests are described.

#### 3.1 Numerical model

The first spray experiments at LUT (Pyy et al., 2015) were performed with the setup, where the spray nozzle was located above a box. CFD model for the arrangement is shown in Figure 5. In the left frame, surface mesh of the CFD model is shown. In the right frame, operation of the spray and flow of liquid film on the floor are illustrated. The mesh has 428 000 hexahedral cells.

In the model, the distance of the spray nozzle from the floor is 100 cm. The height of the box is 60 cm, the length is 120 cm and the width is 80 cm. In the model, the inclination angle of the box floor was 3°. Measurements of droplet sizes with shadowgraphy were made at two positions: 11 cm and 23 cm from the nozzle.

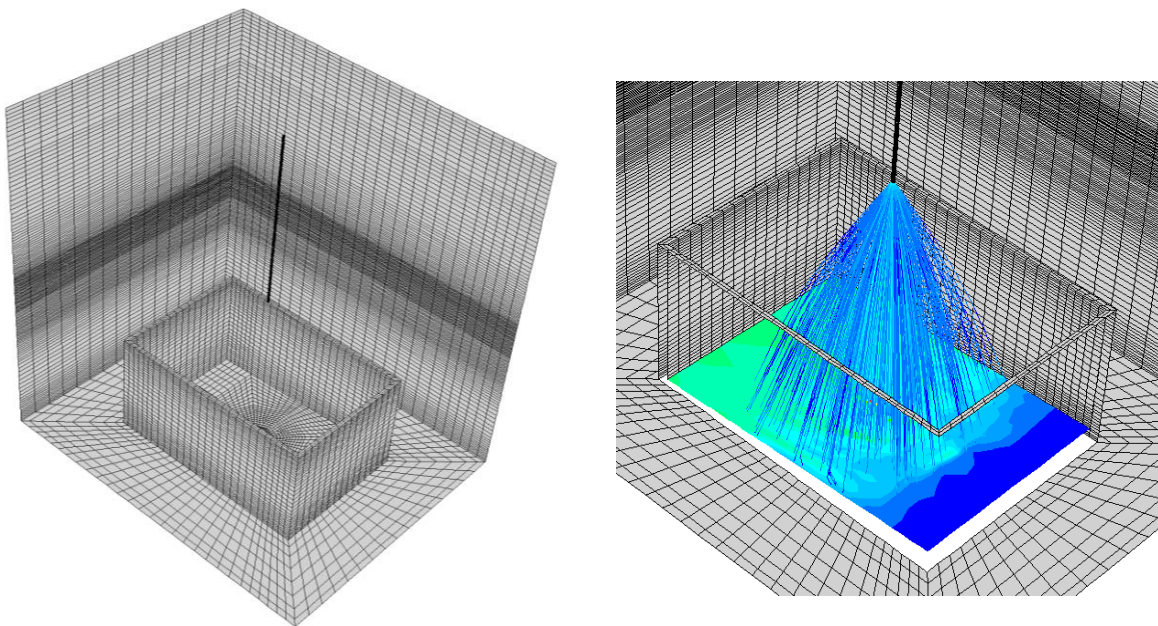


Figure 5. Test arrangement used for preliminary single spray tests (left). The form of the spray and the liquid film on the floor of the box are also shown (right).

Table 3. Properties of the full cone spray nozzle B1/4HH-10 used in the experiments at the preliminary single spray test facility (Spraying Systems Co., 2015).

Nozzle type	Orifice nom. $d$ (mm)	Length $L$ (mm)	$\Delta p$ (bar)	$\dot{V}$ (l/min)	$v = \dot{V}/A$ (m/s)	Cone $\theta/2$
B1/4HH-10	3.2	23	1	4.4	9.12	31.25
			3	7.4	15.3	32.25
			6	10.2	21.1	30.5

In the experiments, three different nozzles were used (see Table 1). In the CFD calculations, the experiment performed with the smallest nozzle B1/4HH-10 was calculated. The experiment, where the pressure difference over the nozzle was 1 bar, was chosen. The mass flow rate at this pressure was 4.4 liters/min and the flow velocity at the exit of the nozzle was 9.12 m/s. The half angle of the cone for this solid cone nozzle is according to the manufacturer 31.25° (Spraying Systems Co, 2015). The parameters of the nozzle are summarized in Table 3.

In the CFD calculations ANSYS Fluent version 16.2 was used. Isothermal calculation was performed, where continuity and momentum equations for gas were solved together with transport equations for turbulence. The turbulence was described with the standard  $k-\varepsilon$  model, where standard wall functions were used with production limiter for the turbulence. The production limiter was used for preventing excessive generation of turbulence at the stagnation point of the flow that is located on the floor of the box. The experiment was performed in a large laboratory, which could not be included in the CFD model. Therefore, only part of the room was model and slip boundary conditions were used for the side walls and the ceiling of the numerical model.

The spray droplets were described with the Discrete Particle Model (DPM) of ANSYS Fluent, where trajectories of the droplets are solved in a numerical mesh. The droplets were assumed to be spherical and the drag included two-way interaction with air. The Rosin-Rammler distribution discussed in Section 2.3 was used for the droplets. The most probable diameter of the droplets was 0.667 mm; the minimum and maximum diameters were 0.05 mm and 1.5 mm, respectively. The spread parameter for the distribution was  $n = 3.5$  (see Figure 4). No breakup or stochastic collisions of the droplets was included in the model.

The full cone model of Fluent was used for the injection of the droplets. The number of the solved droplet trajectories was 300 000, which consisted of 1 000 droplet streams, 30 droplet diameters and 10 tries for stochastic tracking. The stochasticity of the droplet tracks is caused by the interaction of the droplets with turbulence. The solution is iterative, where the two-way momentum transfer between the droplets and air is taken into account.

In the experiments, liquid film was formed on the floor of the box from the spray droplets. In the CFD model, an inclination angle of 3° was assumed for the floor of the box. The flowing liquid film was described with the Eulerian wall film model of ANSYS Fluent. The model solves two-dimensional continuity and momentum equations for the liquid film, which is formed by collection of the spray droplets. The motion of the film is driven by gravity and two-way shear force between the film and air. Stripping of droplets from the film by the shear force was included in the model but splashing caused by droplets was not taken into account. Steady state calculation for the flow of air and droplet trajectories was performed. Simultaneously, transient calculation of the formation and motion of the liquid film was performed with a time step of 0.01 s.

## 3.2 CFD simulations of the preliminary spray experiments

In the following, the results of the simulation of the experiment with nozzle B1/4HH-10 are presented, where the pressure difference over the nozzle was 1 bar (Table 3). The velocity magnitude of droplets is illustrated in Figure 6, where droplets are injected from the nozzle with an initial velocity of 9.12 m/s. The slowing down of the droplets due to the drag caused by air is clearly visible. The smallest droplets flow around with the air and move stochastically due to turbulence.

The flow velocity of air induced by the spray droplets is shown in Figure 7. The strong downwards flow of air in the center of the spray cone can be seen in the left frame. The downward flow turns near the floor of the box and returns upwards near the side walls of the box. In the right frame, the flow velocity of air is shown in one of the measurement planes, which is 23 cm downwards from the spray nozzle.

In Figure 8, concentration of the spray droplets is shown. In the top frame, one can see that the concentration has a strong maximum in the center of the cone. One should note that logarithmic scale is used in the contour plot. In the middle frame, the concentration in a horizontal plane near the floor is shown. The small scale fluctuation of the concentration is caused by the stochasticity of the droplets described with the DPM model.

At the injection, the half angle of the solid cone was defined to be  $31.25^\circ$ . If the half angle of the cone is estimated from the envelope of the concentration shown in the top frame of Figure 8, the result is  $29^\circ$ . The concentration is, however, very small within most of the “solid cone”. In the middle frame of Figure 8, one can see that near the floor the concentration of droplets is very small outside a circle having a radius of 0.3 m. This circle corresponds to a solid cone with half angle of  $17^\circ$ . The concentration of droplets shown in Figure 8 is the property of the injector model of ANSYS Fluent. Currently, experimental concentration data is not available on the spray nozzle B1/4HH-10.

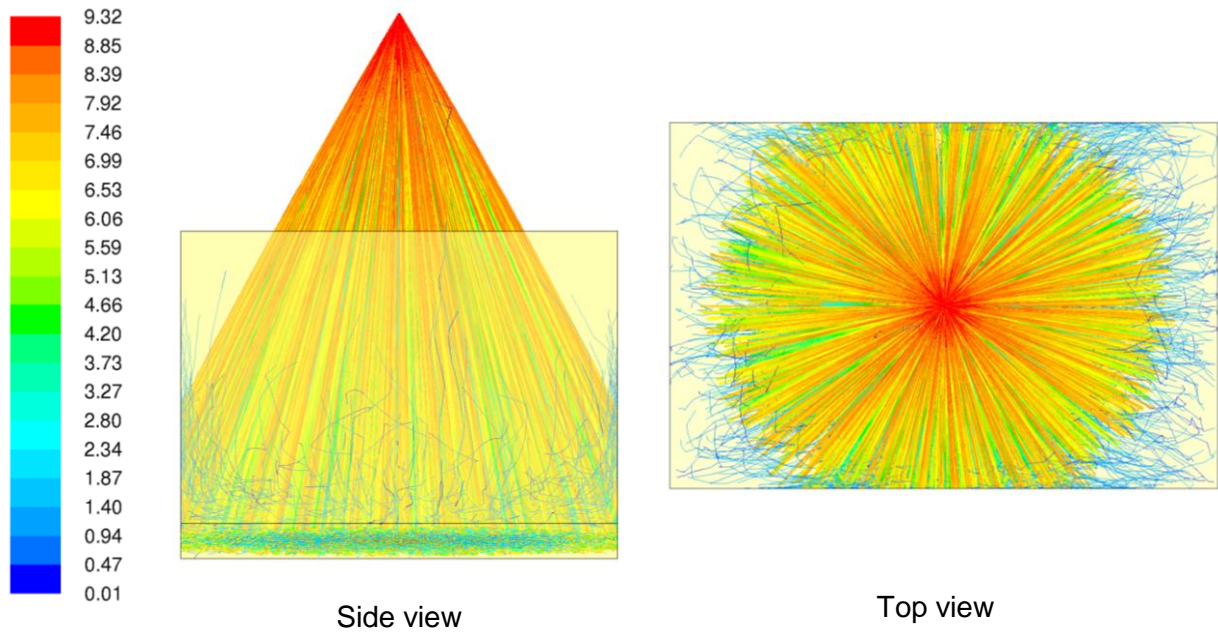


Figure 6. Velocity magnitude of droplets (m/s). Ten percent of the traces of the droplets are shown.

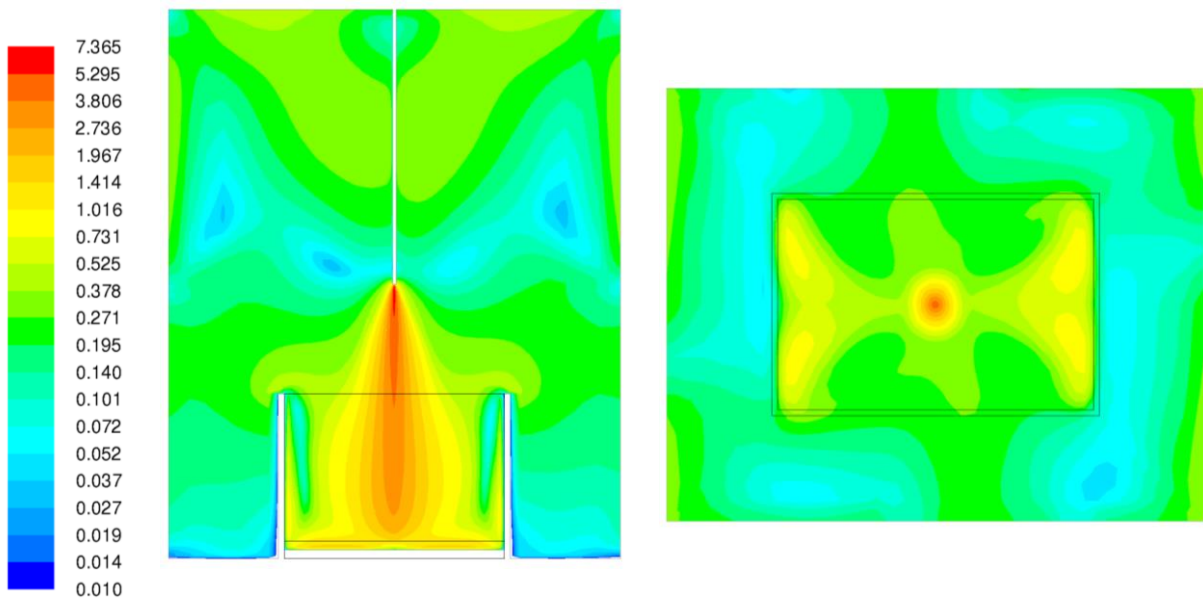


Figure 7. Velocity magnitude of air (m/s) in the vertical center plane through the nozzle (top) and in the horizontal measurement plane 23 cm from the nozzle ( $z = 77$  cm). Note that the velocity scale is logarithmic.

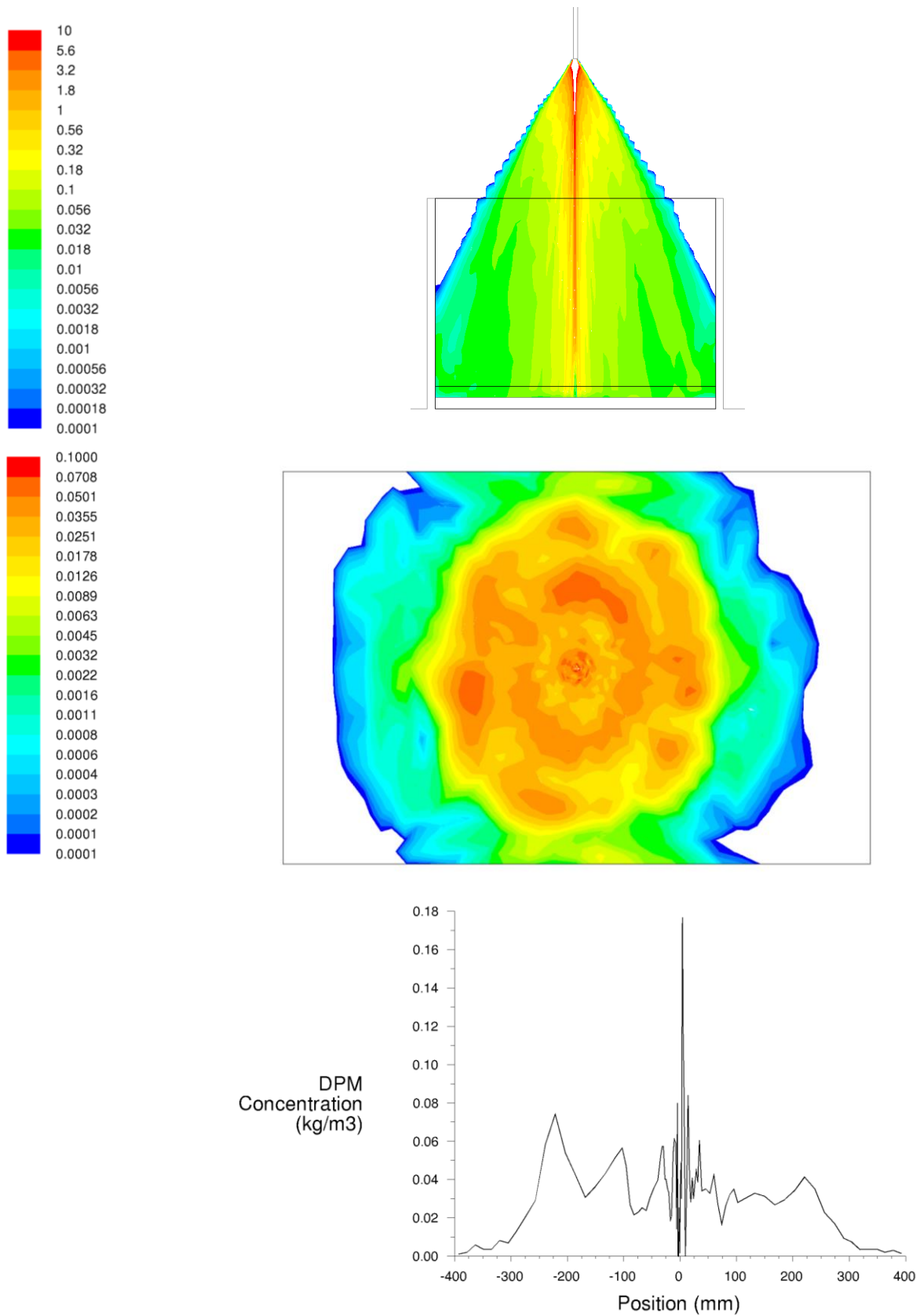


Figure 8. Concentration of droplets ( $\text{kg/m}^3$ ) in the vertical center plane through the nozzle (top) and in the horizontal sampling plane just above the floor (middle). Note that the scales are logarithmic. Concentration is also shown along horizontal line just above the floor (bottom).

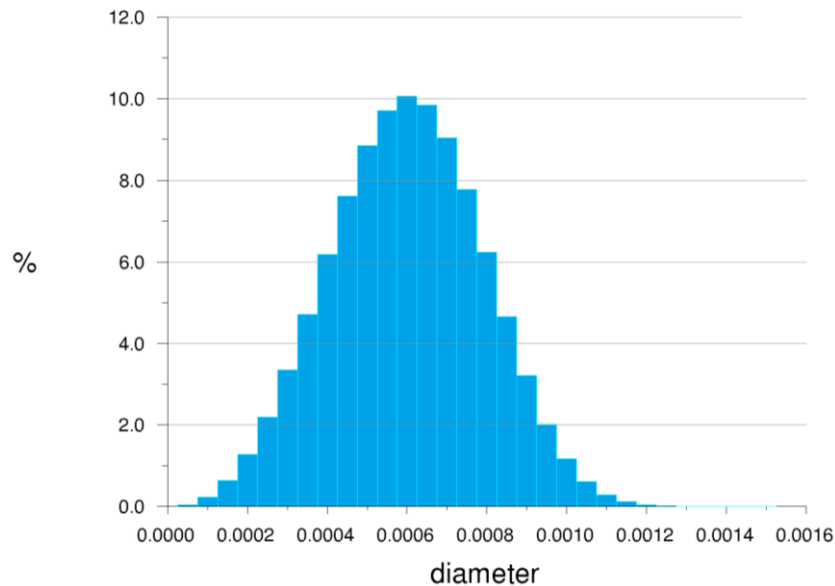


Figure 9. The mass flowrate weighted distribution of droplets versus diameter (m) in the measurement plane 23 cm from the nozzle ( $z = 77$  cm).

In the bottom frame of Figure 8, the droplet concentration is shown along a horizontal line through the center of the spray cone near the floor of the box. Most of the droplets are within a circle having a radius of 0.3 m as was discussed above. Very large local values of the concentration are found in the center of the spray cone. The asymmetry of the concentration is caused by the stochasticity of the droplets described with the DPM model.

Diameter distribution of droplets is shown in Figure 9. The distribution has been obtained by sampling the droplet sizes in the horizontal plane 23 cm from the nozzle, which was one of the measurement planes in the experiment. The average size of the droplets is of the same order as in the experiments (Pyy et al., 2015). Currently, detailed measurement data is, however, not available.

In Figure 10, the thickness and the velocity of liquid film is shown. The thickness and the velocity are determined by the inclination angle of  $3^\circ$  chosen in the numerical model and the shear force caused by the air flowing above the film. The maximum thickness of the film is about 1.1 mm. The typical flow velocity of the film is approximately 10...15 cm/s. The film model was found work qualitatively well with the spray model, when splashing caused by droplets was not included in the calculation.

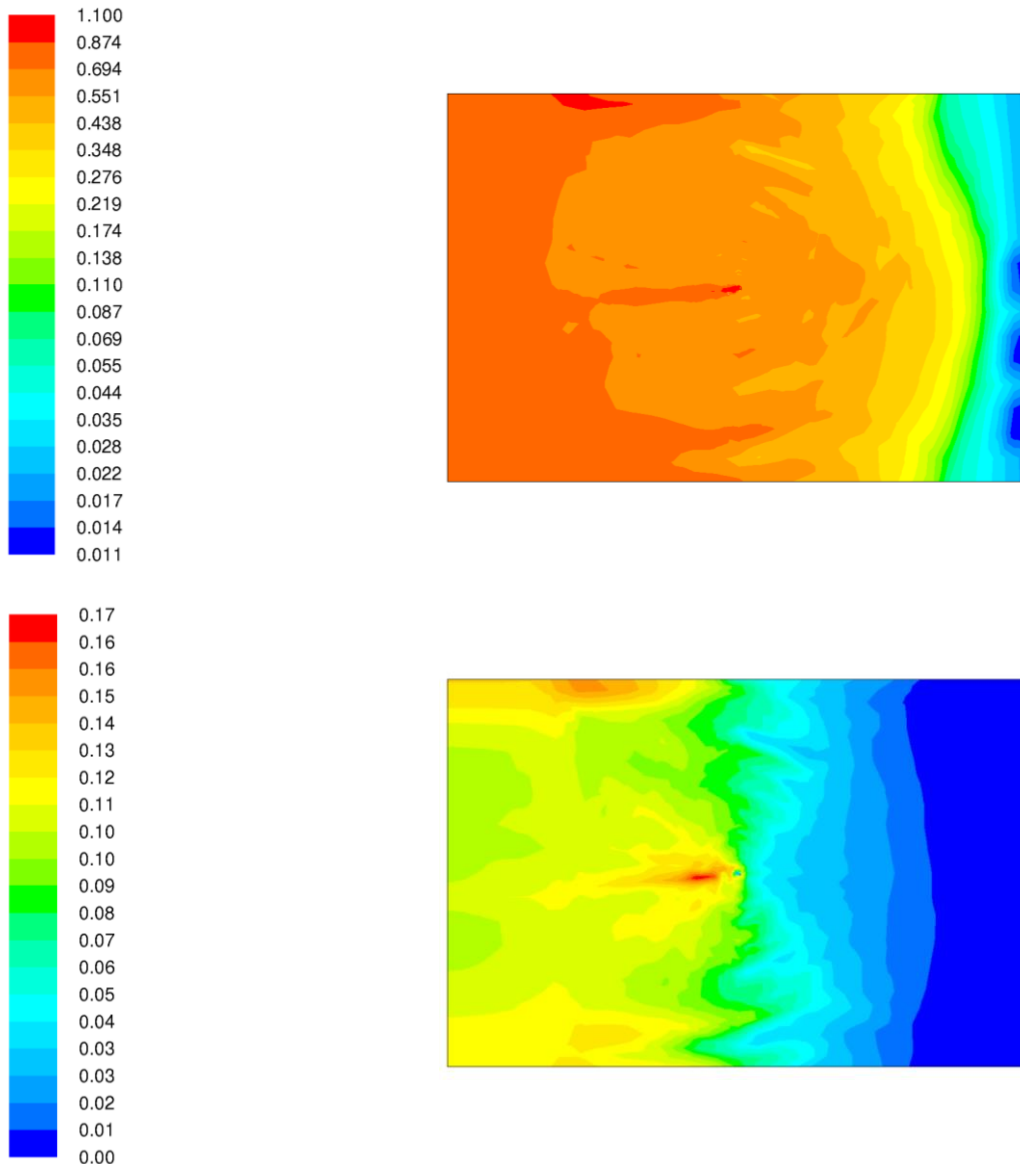


Figure 10. Liquid film thickness (mm) is shown in the top frame and film velocity (m/s) in the bottom frame. The flow direction is from left to right.

## 4. Simulations of the single spray test facility

New single spray test facility was constructed at LUT after performing the preliminary tests (Pyy et al., 2016). At the test facility, series of experiments were performed with the spray nozzle B1/2HH-40, which has the capacity of 40 liters/min (Table 1). CFD calculation of one of the experiments is presented in the following.

### 4.1 Numerical model

CFD model for the new single spray test facility is shown in Figure 11. The distance of the spray nozzle from the floor is 190 cm. The collar of the diffuser used in the measurements is located 110 cm above the floor. Therefore, the distance from the spray nozzle to the measurement position is 80 cm. The diffuser collar is located inside the spray cone so that the end of the collar is located on the cone axis. The hexahedral mesh has 833 000 cells.

In the experiments, the nozzle B1/2HH-40 was used (see Table 1). CFD calculations were performed for the experiment, where the pressure difference over the nozzle was 1 bar. The mass flow rate at this pressure was 17.8 liters/min and the flow velocity at the exit of the nozzle was 9.80 m/s. The half angle of the cone for this solid cone nozzle is according to the manufacturer 44.75° (Spraying Systems Co, 2015). The parameters of the nozzle are summarized in Table 4.

In the CFD calculations ANSYS Fluent version 16.2 was used. The continuity, momentum and energy equations were solved together with transport equations for turbulence. The turbulence was described with the standard  $k-\varepsilon$  model, where enhanced wall treatment was used with production limiter for the turbulence. Slip boundary conditions were used for the side walls and the ceiling of the numerical model. Boundary condition for the temperature on the walls was 20 °C. Initial temperature of the spray droplets was 11 °C.

The spray droplets were described with the DPM model of ANSYS Fluent, where the Rosin-Rammler size distribution discussed in Section 2.3 was used. The most probable diameter of the droplets was 0.713 mm; the minimum and maximum diameters were 0.1 mm and 1.5 mm, respectively. The spread parameter for the distribution was  $n = 3.5$  (see Figure 4). The injection of 300 000 droplets was done similarly as was described in Section 3.1. Formation and flow of liquid film was solved on the floor that had an inclination angle of 5°. In addition, the flow of liquid film on the diffusor collar was calculated.

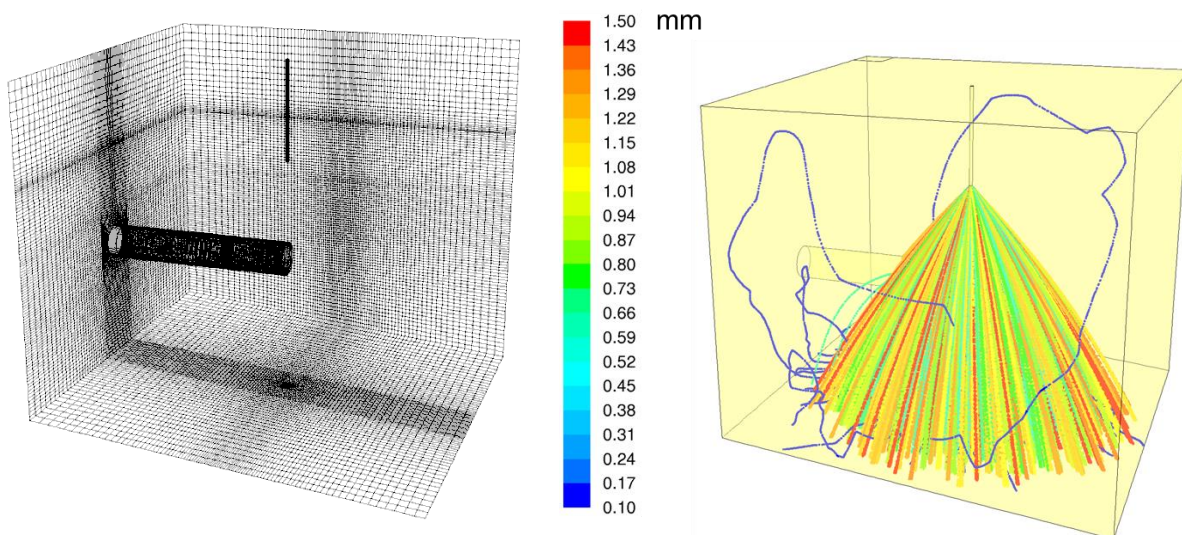


Figure 11. Surface mesh of the CFD model for the spray testing station (left). Model for the experimental arrangement and droplet sizes are also illustrated (right).

Table 4. Properties of the full cone spray nozzle B1/2HH-40 used in the experiments at the single spray test facility (Spraying Systems Co., 2015).

Nozzle type	Orifice nom. $d$ (mm)	Length $L$ (mm)	$\Delta p$ (bar)	$\dot{V}$ (l/min)	$v = \dot{V}/A$ (m/s)	Cone $\theta/2$
B1/2HH-40	6.2	30	1	17.8	9.80	44.75
			6	41	22.63	41.5

## 4.2 CFD simulations of the first experiments

In the following, the results of the simulation of the experiment with nozzle B1/2HH-40 are presented, where the pressure difference over the nozzle was 1 bar (Table 4). The droplet traces colored with diameter are shown in Figure 12, where 30 000 of the total 300 000 traces have been plotted. Some of the smallest droplets are seen to flow around with air in the region of the simulation model. Large droplets are captured by the liquid film on the floor or on the diffuser collar. In the bottom view, one can see that in the numerical model the small droplets are concentrated in the center of the cone. In particular, large amount of small droplets are found below the diffuser collar.

The velocity and thickness of liquid films on the floor and on the diffuser collar are shown in Figure 13. The liquid film on the cylindrical diffuser collar flows downwards along the surface of the collar. On the bottom side of the collar droplets are formed from the liquid film. The droplets fall down to the floor, where they are captured by the liquid film. The maximum velocity of the liquid film on the floor is approximately 22 cm/s. The maximum thickness of the film is about 0.8 mm.

The concentration of droplets is shown in Figure 14. In the injection model, the value of  $44.75^\circ$  was used for the half angle of the solid cone. In the simulation result, one can see that at the distance of 80 cm from the nozzle almost all the droplets are within a circle having a radius of 66 cm. This means that almost all the droplets are within the cone that has half angle of  $40^\circ$ .

Diameter distribution of droplets is shown in Figure 15, which has been obtained by sampling the droplet sizes in the horizontal plane 80 cm from the nozzle. According to preliminary information, the average size of the droplets in the experiments is smaller than the size predicted by the present model (Pyy et al., 2016).

In Figure 16, the velocity magnitude of air is shown. The maximum velocity of air is 7.85 m/s, which is somewhat smaller than the initial velocity of the spray droplets. The maximum velocity of air in front of the collar is approximately 3.8 m/s. The shear force caused by the air passing the collar induces a vortex inside the collar, where the maximum flow velocity of air is 2.5 m/s.

In Figure 17, turbulence kinetic energy and dissipation are shown. As is expected, the turbulence kinetic energy achieves its maximum value inside the spray cone. Some turbulence is also generated inside the diffuser collar. The production limiter used in the turbulence model reduces excessive generation of turbulence in the stagnation points on the diffuser collar and floor. Turbulence dissipation is also strongest in the center of the spray cone and near the floor. Interestingly, the turbulent viscosity ratio ( $\mu_{\text{turb}}/\mu$ ) is strongest on the right side of the spray cone and the viscosity is very unsymmetric.

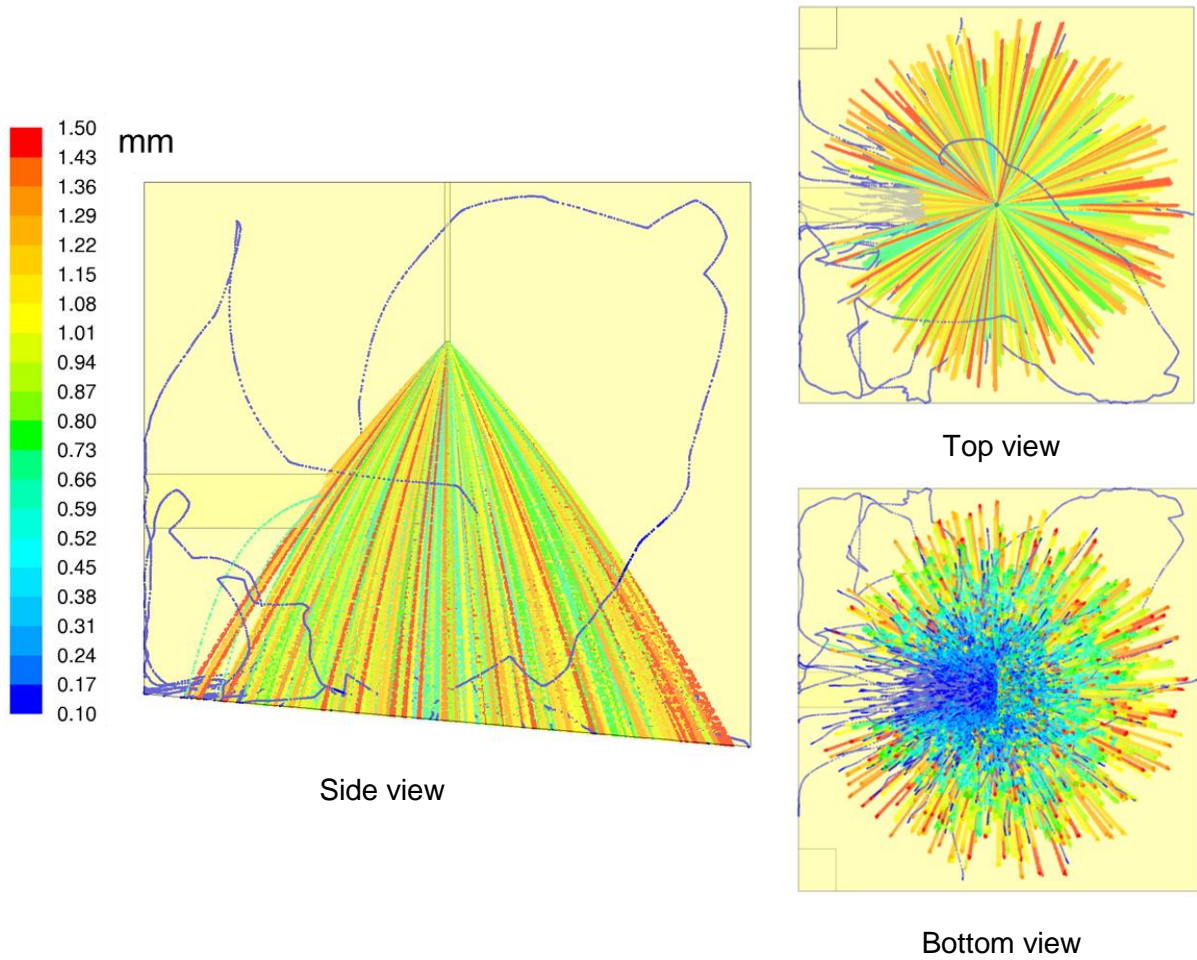


Figure 12. Droplet traces colored with diameter. Ten percent of the traces of the droplets are shown.

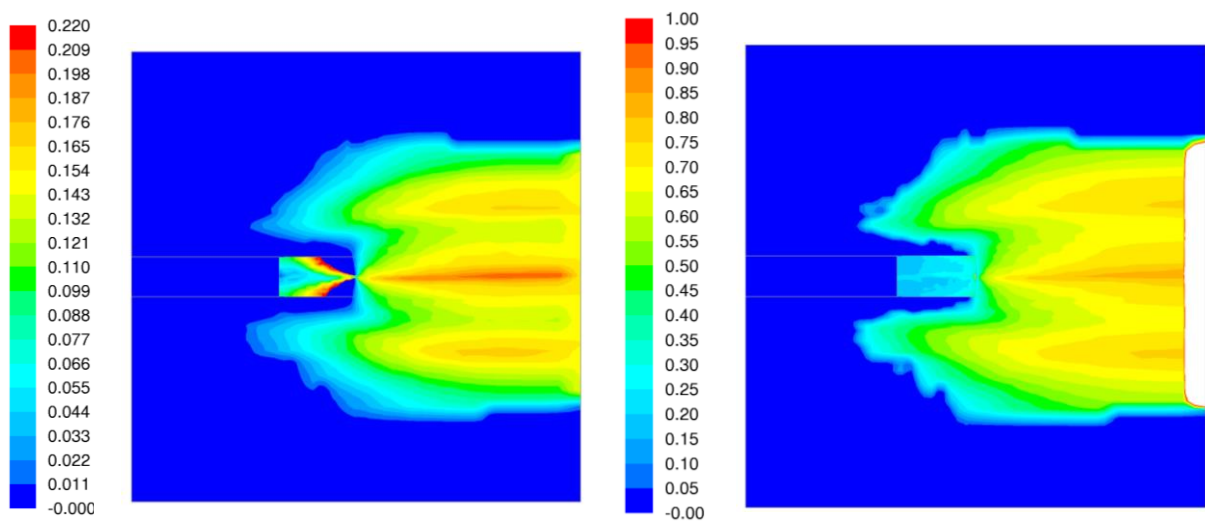


Figure 13. Velocity of liquid film (m/s) on the left and film thickness (mm) on the right. The liquid films on the diffusor collar and on the floor are shown.

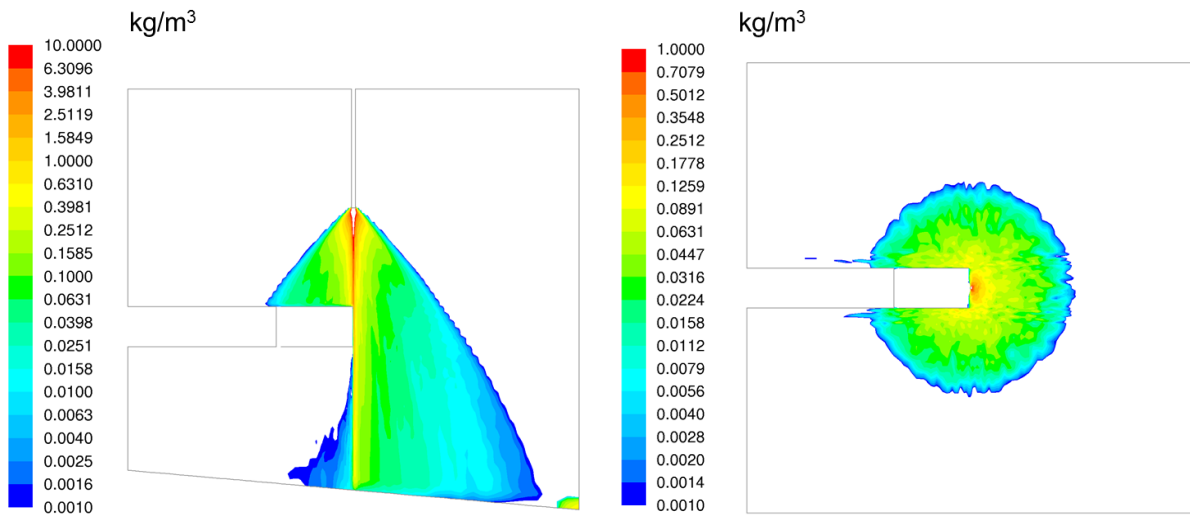


Figure 14. Droplet concentration in the vertical center plane through the nozzle (left) and in the horizontal sampling plane 80 cm from the nozzle ( $z = 110$  cm). Note that logarithmic scale is used.

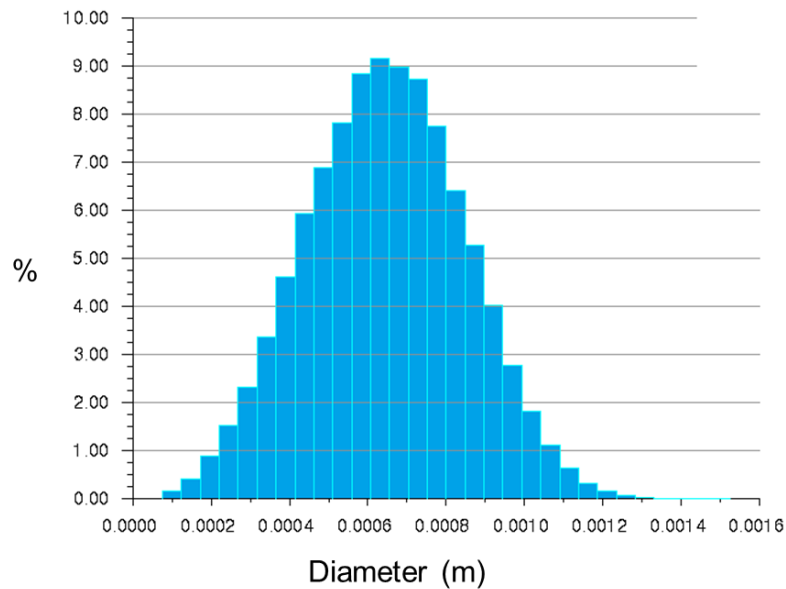


Figure 15. The mass flowrate weighted distribution of droplets on the horizontal measurement plane 80 cm from the nozzle ( $z = 110$  cm).

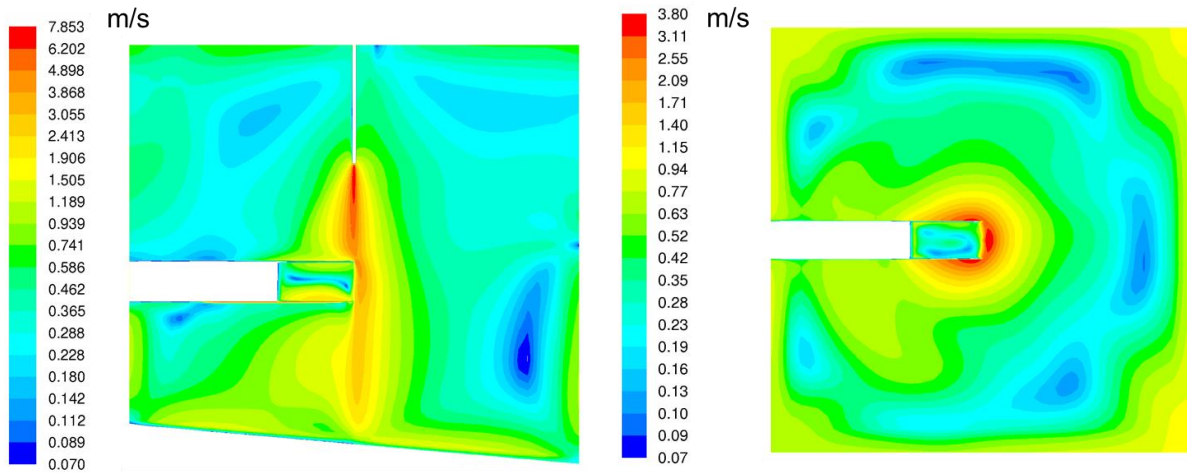


Figure 16. Velocity magnitude of air in the vertical center plane through the nozzle (left) and in the horizontal sampling plane 80 cm from the nozzle ( $z = 110$  cm).

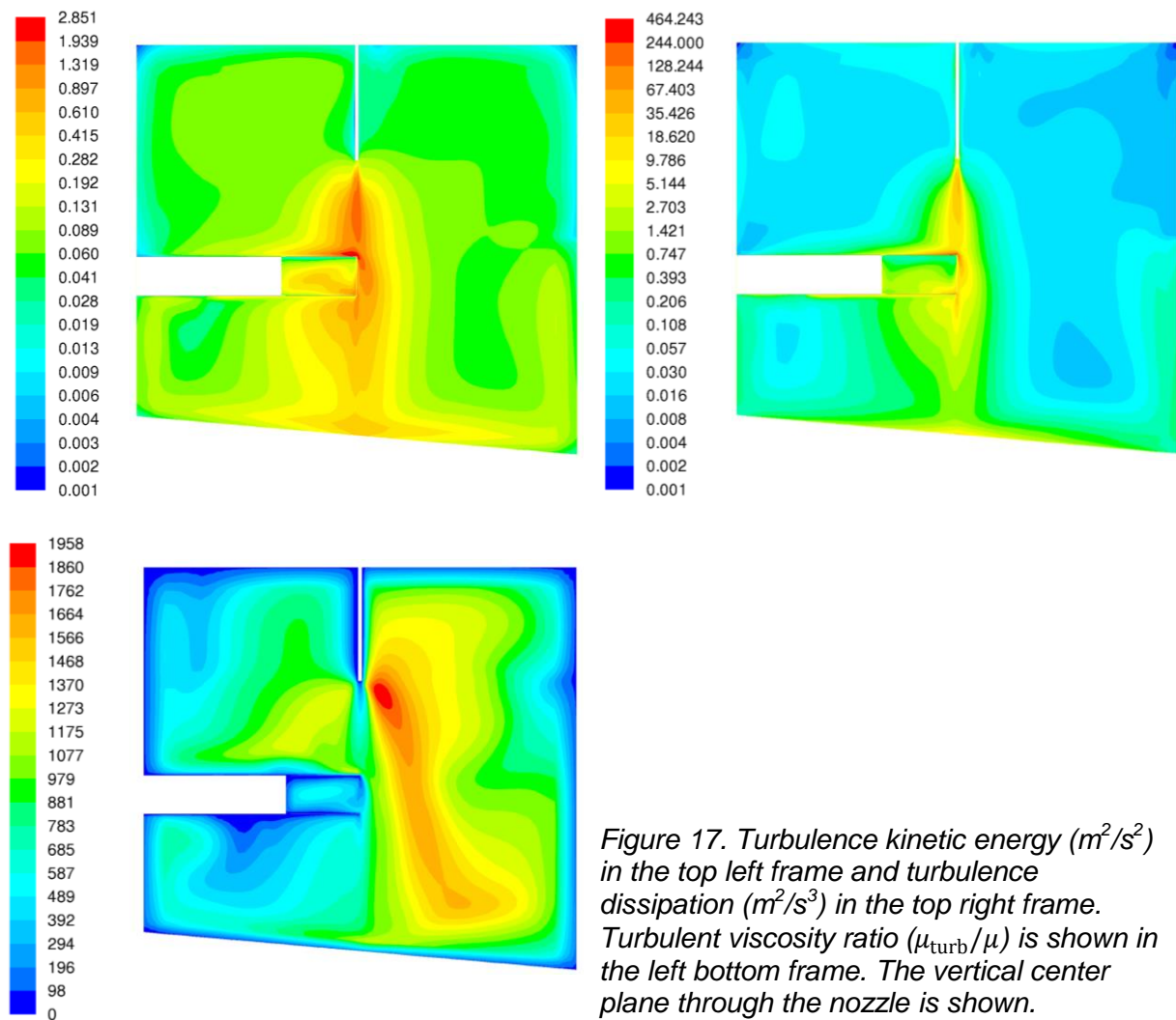


Figure 17. Turbulence kinetic energy ( $m^2/s^2$ ) in the top left frame and turbulence dissipation ( $m^2/s^3$ ) in the top right frame. Turbulent viscosity ratio ( $\mu_{\text{turb}}/\mu$ ) is shown in the left bottom frame. The vertical center plane through the nozzle is shown.

## 5. Summary and discussion

---

Experiments with single spray nozzles are performed at the Lappeenranta University of Technology (LUT). Three different full cone spray nozzles manufactured by Spraying Systems Co (2015) are tested. The size distributions of the droplets are measured with shadowgraphy (Pyy et al., 2015, 2016).

In the present work, the single spray experiments have been modeled with the ANSYS Fluent version 16.2 CFD code. Models for the experimental setups have been constructed and chosen experiments have been simulated by using the Discrete Particle Model (DPM) of Fluent.

The first step in the CFD simulations has been the estimation of droplet size distribution. This has been done by using the plain-orifice model (ANSYS, 2016). The states of the nozzles were first determined by calculating the cavitation numbers of the nozzles. Experiments where the nozzles operate in the single-phase mode were chosen for the simulation. The mean Sauter diameters for the primary breakup distributions of droplets were determined based on the Weber numbers. The Rosin-Rammler distribution was used for the primary breakup distribution of droplets. Values provided by the manufacturer were used for the spray cone angles.

The full cone model of Fluent was used for the injection of the droplets. The number of the solved droplet trajectories was 300 000, which consists of 1 000 droplet streams, 30 droplet diameters and 10 tries for stochastic tracking. The stochasticity of the droplet tracks is caused by the interaction of the droplets with turbulence. The solution was iterative, where the two-way momentum transfer between the droplets and air was taken into account.

First, experiment with the solid cone nozzle B1/4HH-10 (Spraying Systems Co, 2015) was calculated. The nozzle has an orifice with a diameter of 3.2 mm and a capacity of 10 liters/min. The pressure difference over the nozzle was 1 bar and single-phase operation of the nozzle was assumed. The estimate calculated from the plain-orifice model for the Sauter mean diameter of the droplets in the primary breakup distribution was 577  $\mu\text{m}$ . This is roughly of the same order as was observed in the preliminary experiments (Pyy et al., 2015).

Second, an experiment performed at the constructed single spray testing station was calculated. The larger solid cone spray nozzle B1/2HH-40 (Spraying Systems Co, 2015) was used in the experiment. This nozzle has an orifice with a diameter of 6.2 mm and a capacity of 40 liters/min. The pressure difference over the nozzle was also in this case 1 bar and single-phase operation of the nozzle was assumed. The estimate for the Sauter mean diameter of the droplets in the primary breakup distribution was 617  $\mu\text{m}$ . Preliminary information from the experiments suggests that the real value is smaller (Pyy et al., 2016).

After the primary breakup of the spray, additional breakup of droplets may occur. Several models exist for this so-called secondary breakup. The simplest model available in ANSYS Fluent is the Taylor Analogy Breakup (TAB) model, which compares the surface tension forces of the droplet to the drag force caused by surrounding air (ANSYS, 2016; Chryssakis et al., 2011). This model is only suitable for small Weber numbers ( $We < 100$ ). An alternative to TAB model is the Wave Breakup Model, where the fastest-growing Kelvin-Helmholtz instability for the spray jet is determined (ANSYS, 2016; Chryssakis et al., 2011). The wavelength and growth rate of the instability determine the sizes of the droplets.

After the primary breakup of the spray jet, the secondary breakup of droplets may further reduce their mean diameter. The secondary breakup was, however, not included in the present CFD model. It's possible inclusion could affect the results of the simulations, where the distance of the measurement plane from the spray nozzle is large. Such a situation occurred in the simulation of Section 4, where the distance was 80 cm. In the simulations of Section 3, the distance was only 23 cm. The significance of the secondary breakup at

different distances from the nozzle should be revealed by further analysis of the experimental data.

The collisions and the coalescence of the droplets were not considered in the present analysis. In ANSYS Fluent (ANSYS, 2016), the collision method proposed by O'Rourke (1981) is available. The collision of droplets located in the same grid cell is modeled based on the collisional Weber number, where relative velocity of the droplets is used. As the result of the collision, bouncing or coalescence of the droplets may occur. The importance of the collisions for the present simulations is not clear and should be further studied.

As the result of the present simulations, the concentration of droplets in different regions of the spray cone was obtained. In addition, it was observed that large amount of small droplets were located near the axis of the spray cone. More detailed comparison of these observations to forthcoming experiments will be of interest.

## References

---

- ANSYS Inc., 2016. ANSYS Fluent Theory Guide, Release 17.0, Section 16.12, Atomizer model theory, USA.
- Brennen, C.E., 2005. Fundamentals of Multiphase Flow, Section 12: Sprays, Cambridge University Press, New York, USA.
- Chryssakis, C.A., Assanis, D.N. and Tanner, F.X., 2011. Atomization Models, in Handbook of Atomization and Sprays, Ed. N. Ashgriz, Springer, New York, USA.
- Foissac, A., Malet, J., Vetrano, M.R., Buchlin, J.-M., Mimouni, S., Feuillebois, F. and Simonin, O., 2011. Droplet size and velocity measurements at the outlet of a hollow cone spray nozzle, *Atomization and Sprays* **21**, 893–905.
- Lefebvre, A.H., 1989. *Atomization and Sprays*, Hemisphere.
- O'Rourke, P.J., 1981. *Collective Drop Effects on Vaporizing Liquid Sprays*, PhD thesis. Princeton University, New Jersey, USA.
- Pyy, L., 2015. First experiments with spray nozzles, private discussion in December 2015.
- Pyy, L., 2016. Experiments with single spray testing station, private discussion in January 2016.
- Sazhin, S., 2014. *Droplets and Sprays, Section 2: Spray Formation and Penetration*, Springer, London.
- Schick, R.J., 2006. *Spray technology reference guide: Understanding drop size*, Spraying Systems Co., Bulletin No. 459B, USA 35 p.
- Spraying Systems Co, 2015. Full cone spray nozzles, [http://www.spray.com/spray\\_nozzles/standard\\_spray\\_nozzles.aspx](http://www.spray.com/spray_nozzles/standard_spray_nozzles.aspx).
- Wu, P.-K., Tseng, L.-K. and Faeth, G.M., 1992. Primary breakup in gas/liquid mixing layers for turbulent liquids, *Atomization and Sprays* **2**, 295-317.

Title	CFD simulations of preliminary single spray experiments
Author(s)	Timo Pättikangas and Risto Huhtanen
Affiliation(s)	VTT Technical Research Centre of Finland
ISBN	978-87-7893-451-2
Date	June 2016
Project	NKS-R / COPSAR
No. of pages	25
No. of tables	4
No. of illustrations	17
No. of references	12
Abstract max. 2000 characters	The single spray nozzle experiments performed at the Lappeenranta University of Technology (LUT) are modelled with CFD calculations. The spray droplets are described by using the Discrete Particle Model of the ANSYS Fluent code. Suitable model for the size distribution of the droplets is chosen from the models available in Fluent. Single spray nozzle experiments performed at LUT are modelled and the CFD calculations are compared to available experimental results. The results will be used for the modelling of the spray experiments performed with the PPOOLEX facility at LUT.
Key words	Spray, droplet, containment, nuclear reactor safety, NRS, computational fluid dynamics, CFD